Analytica Chimica Acta 844 (2014) 27–34

Contents lists available at ScienceDirect

Analytica Chimica Acta

journal homepage: www.elsevier.com/locate/aca

A capacitive biosensor based on an interdigitated electrode with nanoislands

Ha-Wook Jung [a,1], Young Wook Chang [a,1], Ga-yeon Lee [a], Sungbo Cho [b], Min-Jung Kang [c], Jae-Chul Pyun [a,*]

[a] Department of Materials Science and Engineering, Yonsei University, 134 Shinchon-dong, Seodaemun-gu, Seoul 120-749, South Korea
[b] Department of Biomedical Engineering, Gachon University, Incheon 406-799, South Korea
[c] Korea Institute of Science and Technology (KIST), Seoul, South Korea

HIGHLIGHTS

- An interdigitated electrode (IDE) with nanoislands was developed for capacitive biosensor.
- The sensitivity of capacitive immunoassay could be enhanced by the IDE with nanoislands.
- A parylene film was coated on the IDE to improve the immobilization efficiency of receptors.
- The parylene film coated electrode was applied to detect hepatitis surface antigen (hHBsAg).

GRAPHICAL ABSTRACT

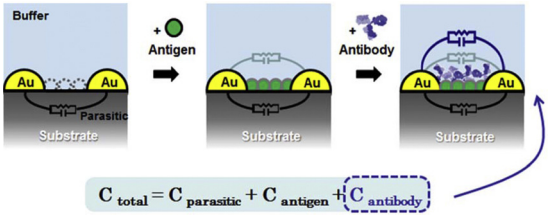

ARTICLE INFO

Article history:
Received 31 January 2014
Received in revised form 1 July 2014
Accepted 8 July 2014
Available online 11 July 2014

Keywords:
Interdigitated electrode
Nanoisland
Capacitive biosensor
Hepatitis B virus
Surface antigen
Immunosensor

ABSTRACT

A capacitive biosensor based on an interdigitated electrode (IDE) with nanoislands was developed for label-free detection of antigen-antibody interactions. To enable sensitive capacitive detection of protein adsorption, the nanoislands were fabricated between finger electrodes of the IDE. The effect of the nanoislands on the sensitive capacitive measurement was estimated using horseradish peroxidase (HRP) as a model protein. Additionally, a parylene-A film was coated on the IDE with nanoislands to improve the efficiency of protein immobilization. By using HRP and hepatitis B virus surface antigen (HBsAg) as model analytes, the effect of the parylene-A film on the capacitive detection of protein adsorption was demonstrated.

1. Introduction

Capacitive biosensors based on interdigitated electrodes (IDE) have been of interest for non-labeled detection of interactions between biomolecules because of their high sensitivity and their relative simplicity [1–8]. Recently, capacitive biosensors based on IDE have been reported for the detection of C-reactive protein (CRP) [9], IL-6 [10], CEA [11], Johne's disease specific antigen [12], Hev b1 [13], and Nampt [14], as summarized in Table 1. The capacitive detection of IDE is based on the following equation of capacitance: $C = \varepsilon_0 \times \varepsilon_r \times A \times d^{-1}$, where ε_0 and ε_r represent vacuum permittivity and the relative permittivity of a dielectric material between electrodes, respectively, and where d and A represent

* Corresponding author. Tel.: +82 2 2123 5851; fax: +82 2 365 5882.
E-mail address: jcpyun@yonsei.ac.kr (J.-C. Pyun).
[1] These two authors contributed equally to this work.

http://dx.doi.org/10.1016/j.aca.2014.07.006
0003-2670/

Table 1
Comparison of sensing parameters of capacitive biosensors based on IDEs.

Authors	Target analyte	Linear range (ng mL^{-1})	Limit of detection
Kallempudi and Gurbuz 2011 [9]	CRP	1 ~ 250	1 ng mL^{-1}
Qureshi et al., 2010 [10]	IL-6	0.025 ~ 25	25 pg mL^{-1}
Altintas et al., 2014 [11]	CEA, hEGR	0.02 ~ 1	20 pg mL^{-1}
Li et al., 2014 [12]	Anti-bovin IgG	–	1 ng mL^{-1}
Sontimuang et al., 2011 [13]	Hev b1	10 ~ 900	10 ng mL^{-1}
Park et al., 2012 [14]	Nampt	1 ~ 50	1 ng mL^{-1}
(This work)	HBsAg	0.1 ~ 1000	<100 pg mL^{-1}

electrode distance and area, respectively. As the relative permittivity of a protein ($\varepsilon_r = 20$) is significantly different from that of water ($\varepsilon_r = 80$), a change in capacitance can occur due to the adsorption of proteins on the electrodes. The equation above shows that the change in capacitance is enhanced if the distance between the electrodes is shortened. Therefore, IDE have been developed to minimize the distance between the finger electrodes for sensitive capacitive detection. In previous studies [9–14], most IDE have been fabricated with UV-photolithography with a linewidth limit of 1–5 μm [15]. The IDE-type electrodes with a < 1 μm distance between the finger electrodes are known to require costly and time-consuming processes such as E-beam lithography [16], focused ion-beam fabrication [17], and a mass-producible submicron-gap IDE via step photolithography [18]. In addition to the IDE, nanoislands have also been applied to the capacitive detection of proteins by fabrication with field effect transistor (FET) devices and Pt-carbon nanotube electrodes [19–22]. Such nanoislands have been fabricated with various methods such as thermal annealing, intense pulsed light, nanoporous alumina blocks, and e-beam evaporation [19–21,23]. In this work, IDE with nanoislands were fabricated between the finger electrodes of an IDE in order to shorten the distance between the finger electrodes of the IDE, as shown in Fig. 1(a). From the simulation results, analysis of the nanoislands determined that they concentrated the electric fields on IDE far higher than the conventional IDE, which had widely distributed electric fields into the electrolytes. The improvement in sensitivity of the IDE with nanoislands in detecting the changes in capacitance and impedance was demonstrated using model analytes in comparison with the conventional IDE.

The creation of such an IDE with nanoislands aimed to improve the sensitivity in the measurement of impedance and capacitance during immunoassays. For highly sensitive immunoassays, the receptor proteins (antibodies or antigens) should be immobilized on the sensor surface with a high surface density. Recently, parylene films with functional groups such as amines and formyl groups were reportedly used for the covalent immobilization of proteins and peptides for highly sensitive immunoassays. Among such parylene films with functional groups, parylene-A is a polymer of *p*-xylene with primary amine groups, which can be used for the covalent binding of proteins or peptides with linker molecules such as glutaraldehyde or succinimide derivatives [24]. In particular, parylene-A was used for the immobilization of small proteins and peptides and achieved a far higher efficiency than using physical adsorption and self-assembled monolayers [25]. In this work, parylene-A was applied to the IDE with nanoislands to enhance the sensitivity of immunoassays. For application to the IDE with nanoislands, the parylene-A film should be coated as thin as possible (<50 nm) to achieve the sensitive capacitive detection by on-line thickness monitoring [26–29].

Here, the fabrication of the IDE with nanoislands is presented, and the morphological analysis of nanoislands was carried out by scanning electron microscopy (SEM) and atomic force microscopy (AFM). The effect of nanoislands on the sensitive capacitive measurement was characterized by immunoassays with horseradish peroxidase (HRP) as a model protein. Then, a parylene-A film was coated on the IDE with nanoislands to enhance the sensitivity of capacitive detection, and immunoassays with the parylene-A coated electrode were conducted using HRP and hepatitis B virus surface antigen (HBsAg) as model analytes.

2. Materials and methods

2.1. Materials

Horseradish peroxidase (HRP), an anti-HRP antibody, ferricyanide, and other chemicals of analytical grade were purchased from Sigma–Aldrich Korea (Seoul, South Korea). Hepatitis B virus surface antigen (HBsAg) and anti-HBsAg antibodies were purchased from AbCam Co (Cambridge, UK).

2.2. Fabrication of an IDE with nanoislands

The IDE was fabricated on a glass substrate using a UV-photolithographic process, shown in Fig. 1(b). For the fabrication of the IDE, a SU-8 layer of 1 μm thickness was spin-coated on a 4-inch glass wafer. After soft-baking at 110 °C for 2 min, the UV-photolithography process was carried out using a mask for the IDE. The IDE was designed to have 100 pairs of finger electrodes with a width of 5 μm, and the space between electrodes was set to be 5 μm. After developing the IDE pattern, a Ti layer was sputtered as an adhesive layer with a thickness of 5 nm, and then a gold layer was sputtered with a thickness of 100 nm. The IDE pattern was obtained after a lift-off process. Nanoislands were prepared on the IDE by thermal evaporation and heat treatment. First, the gold layer was thermally evaporated with a thickness of 1 nm, and then nanoislands were produced by heat treatment under argon gas (150 sccm) at a temperature of 500 °C for 1 h. Additionally, the surface density of nanoislands was controlled by thermal annealing of the gold layers with different thicknesses of 2, 5, 8 nm which resulted in the surface density of 1.1×10^9, 6.6×10^8 and 7.8×10^7 nanoislands cm^{-2}, respectively.

2.3. Thermal deposition of the parylene-A film

As previously reported, parylene-A (Femto Science Co., South Korea) was thermally deposited by the following polymerization steps: (1) evaporation of parylene dimers at a temperature of 160 °C, (2) pyrolysis for the production of highly reactive *p*-xylene radicals at a temperature of 650 °C, and (3) deposition of the parylene-A film to the substrate at room temperature [26–29]. The whole coating procedure was reproducibly carried out using a microprocessor-controlled parylene coater from Femto Science Co. (South Korea). To control the thickness of the parylene-A film, the QCM response was measured from the beginning of the evaporation step, and the thermal deposition was finished when the QCM frequency shift reached a value corresponding to the targeted thickness of the parylene-A film [29,30].

2.4. Protein immobilization

For the immobilization of proteins (HRP and HBsAg), 5% glutaraldehyde in phosphate buffered saline (pH 7.0) was applied to the parylene-A film for 1 h at 37 °C. After washing with PBS, the protein solution at concentrations between 100 ng mL^{-1} and 1 μg mL^{-1} was applied for 1 h at 37 °C. After the incubation step, the sensor surface was washed with 1% Tween 20 [29,30]. In the case of protein immobilization to the bare gold electrodes, the proteins (HRP and HBsAg) and glutaraldehyde in phosphate buffered saline (pH 7.0) were immobilized through physical adsorption by incubation for 1 h at 37 °C.

2.5. Electrochemical measurements

Cyclic voltammetry (CV) was performed using a potentiostat from IVIUM Technologies (Compactstat, Netherlands). For characterization of the nanoislands, a three-electrode system was prepared using the IDE with nanoislands as a working electrode. An external reference electrode of Ag/AgCl and a counter electrode

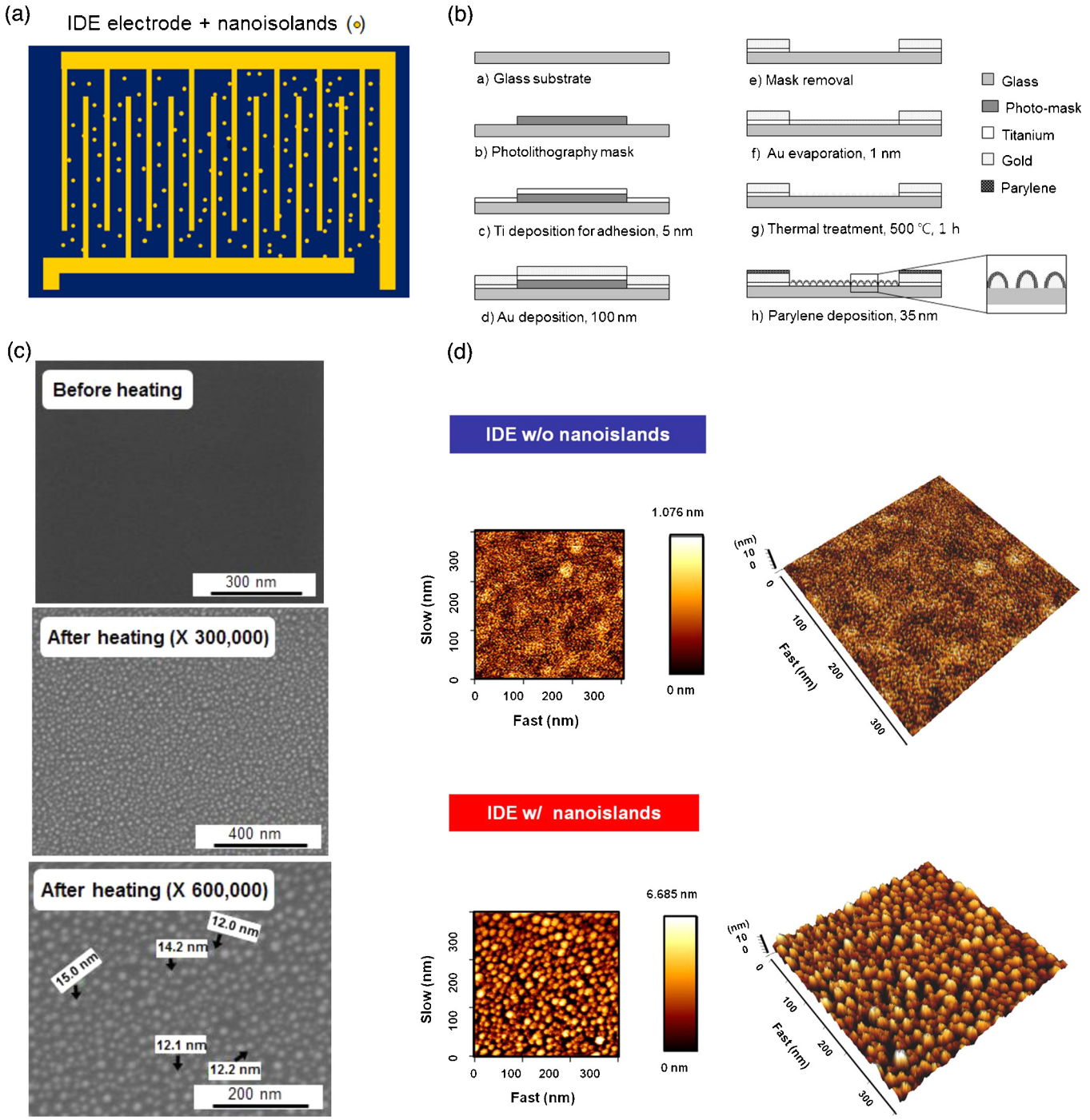

Fig. 1. Interdigitated electrode (IDE) with nanoislands. (a) Schematic view of the IDE with nanoislands. (b) Fabrication method of the IDE with nanoislands. After IDE fabrication by a standard UV-photolithography process, nanoislands were produced by thermal evaporation of a gold layer (1 nm) and heat treatment (500 °C, 1 h). (c) SEM images of the gold surface before (left) and after (center and right) thermal treatment. (d) AFM images of the IDE with and without nanoislands.

made of Pt-wire were used for the analysis of a well-known redox couple of 10 mM ferricyanide ($Fe(CN)_6^{3-/4-}$). The cyclic voltammogram (CV) of the ferricyanide sample was obtained in a potential range from −300 to +500 mV (versus Ag/AgCl) at a scanning rate of 30 mV s^{-1}. Impedance measurements were also performed using a potentiostat from IVIUM Technologies (Compactstat, Netherlands). The impedance was measured in a frequency range from 20 Hz to 1 kHz with an applied potential of 100 mV [29].

3. Results and discussion

3.1. Properties of the electrodes with nanoislands

Nanoislands were fabricated on the IDE by (1) deposition of a gold layer with a thickness of 1 nm and (2) thermal treatment for 1 h at 500 °C. The size and distribution of the nanoislands were determined by the thermal treatment conditions. As shown in Fig. 1(c), circular-type nanoislands with an average diameter of 13 nm ($n = 15$) were obtained by the thermal treatment under argon gas (150 sccm) for 1 h at 500 °C. From the analysis of SEM images, the distribution of nanoislands was estimated to be homogeneous on the electrode surface with a surface density of 6×10^{11} nanoislands cm^{-2}. The three-dimensional structure of the nanoislands was analyzed using AFM (Bio-AFM from JPK Co., USA). As shown in Fig. 1(d), the roughness (R_q) of the gold electrode of the IDE was estimated to be 0.237 nm, and the roughness (R_q) was changed to 1.519 nm after fabrication of the nanoislands. From the topological analysis of AFM images, the nanoislands seem to have a half-spherical shape, and the distribution was observed to be on the IDE surface. Similar to the SEM analysis, AFM analysis determined the distribution of nanoislands to be homogeneous on the electrode surface with a surface density of 2×10^{11} nanoislands cm^{-2}. Additionally, the influence of the nanoisland fabrication conditions on the capacitance of the electrode was estimated by preparing nanoislands with gold layers of two different thicknesses (0.5 nm and 1 nm) and testing three different thermal treatment conditions (300, 500, 700 °C). As shown in Supplement 1, the maximum capacitance was observed at the gold layer with a thickness of 1 nm and the thermal treatment at a temperature of 500 °C. From these results, the nanoislands on the IDE were prepared using a gold layer with a thickness of 100 nm and a thermal treatment at a temperature of 500 °C. When the surface density of nanoislands was controlled to be 1.1×10^9, 6.6×10^8 and 7.8×10^7 nanoislands cm^{-2} from the gold layers with thicknesses of 2, 5, 8 nm, respectively (Supplement 2(a)). As thickness of the gold layer before thermal annealing was increasing, the difference in the size of nanoislands was observed to be increased. The impedance measurement with the IDEs of controlled surface densities of nanoislands showed the decrease of impedance value at the low frequency range of less than 10 kHz under PBS (Supplement 2(b)). These results clearly represented the influence of surface densities of nanoislands on the impedance between electrodes.

3.2. Immunoassays with the IDE with nanoislands

A capacitive change is known to occur when proteins are adsorbed between the finger electrodes of the IDE. Usually, the protein adsorption does not make a completely homogeneous dielectric layer, and the resistance component (R) should always be connected in parallel with a capacitor (C). The immunoassay was carried out using the IDE with nanoislands as shown in Fig. 2(a), and the analytes (antigens or antibodies) were sequentially layered on the receptor molecule (antibodies or antigens) at each step of the immunoassay. As such, an adsorption of proteins on the electrode could be regarded as a parallel connection of capacitors. The change in capacitance was obtained as the sum of the capacitive components including the parasitic capacitance of the electrode, and the capacitance increased with the adsorption of proteins.

The nanoislands were fabricated to improve the sensitivity of the IDE. To estimate the effect of the nanoislands, the capacitive change of IDE with and without nanoislands was measured with standard salt solutions at different concentrations. As shown in Fig. 2(b), the capacitance of the standard salt solutions at a concentration range of 0.5–3.0% was 19.3–24.7 nF for the IDE without nanoislands. In the case of the IDE with nanoislands, the capacitance ranged from 43.6 to 68.5 nF at the same concentration range. The linear correlation between the standard salt concentration at a range of 0.5–3.0% and the capacitive change was estimated to be 2.0 nF/% of salt concentration using the IDE without nanoislands and 10.1 nF/% of salt concentration using the IDE with nanoislands. Therefore, the capacitance change was far more sensitive when using the IDE with nanoislands compared with the IDE without nanoislands, and the change in capacitance measured was far larger than the impedance change using the IDE with nanoislands.

The immunoassay was carried out using the IDE with nanoislands and HRP as a model analyte. The effect of the nanoislands for IDE was estimated by comparing immunoassay results from IDE with and without nanoislands. As a first step, HRP was immobilized on both IDE by physical adsorption, and the sites of non-specific binding on the electrodes were blocked by treatment with BSA at a concentration of 10 mg mL^{-1}. Then, both IDE were treated with standard anti-HRP antibodies. As shown in Fig. 2(c), the capacitive change was 0.4–0.8 nF (Δcapacitance = 0.4 nF) for the IDE without nanoislands. In the case of the IDE with nanoislands, the capacitive change was measured to be from 29.7 to 44.6 nF (Δcapacitance = 14.9 nF). These results showed that the capacitive measurement associated with the immunoassay had a far higher sensitivity using the IDE with nanoislands than the IDE without nanoislands. The reproducibility of capacitance measurements was estimated for IDE electrodes with nanoislands after the protein adsorption using three different electrodes. The capacitance change from PBS was compared after the immobilization of HRP at the concentration of 100 μg mL^{-1} in PBS, and the results of capacitance measurement at the frequency of 100 Hz was estimated to be 122 ± 11 (9%) nF ($n = 3$). At the frequency of 1 kH, the reproducibility of capacitance measurement after the immobilization of HRP was estimated to be 87 ± 10 (11%) nF ($n = 3$). These results showed that the device-to-device reproducibility of capacitive measurements for each IDE with nanoislands was estimated to be around 10% at the frequency of 100 Hz and 1 kHz, respectively.

The sensitivity of the impedance measurement to the protein on the IDE is involved with the distribution of the electric fields over the proteins, which can be determined by the electrode area and configuration. In the case of the normal IDE, the electrical properties of the protein adsorbed on the electrode affect the current flow between the IDE more and change the measured impedance as the spacing between the fingers of IDE decreases [31,32]. The fabricated IDE with nanoislands induces the increase in the current density and the electrical field on the protein adsorbed on the nanoislands. When an input potential of 10 mV with a frequency of 1 kHz was applied, the electrical fields and current density around a finger of the IDE with or without nanoislands with protein adsorbed onto them were simulated using the finite element method and shown in Fig. 2(d). The IDE finger model was designed to have a thickness of 100 nm and a protein layer homogeneously coated on the surface of both the electrode and the nanoislands with a thickness of 5 nm. The nanoislands had a radius of 7 nm and a center to center distance of 44 nm. For the simulation, it was assumed that the conductivity (σ)

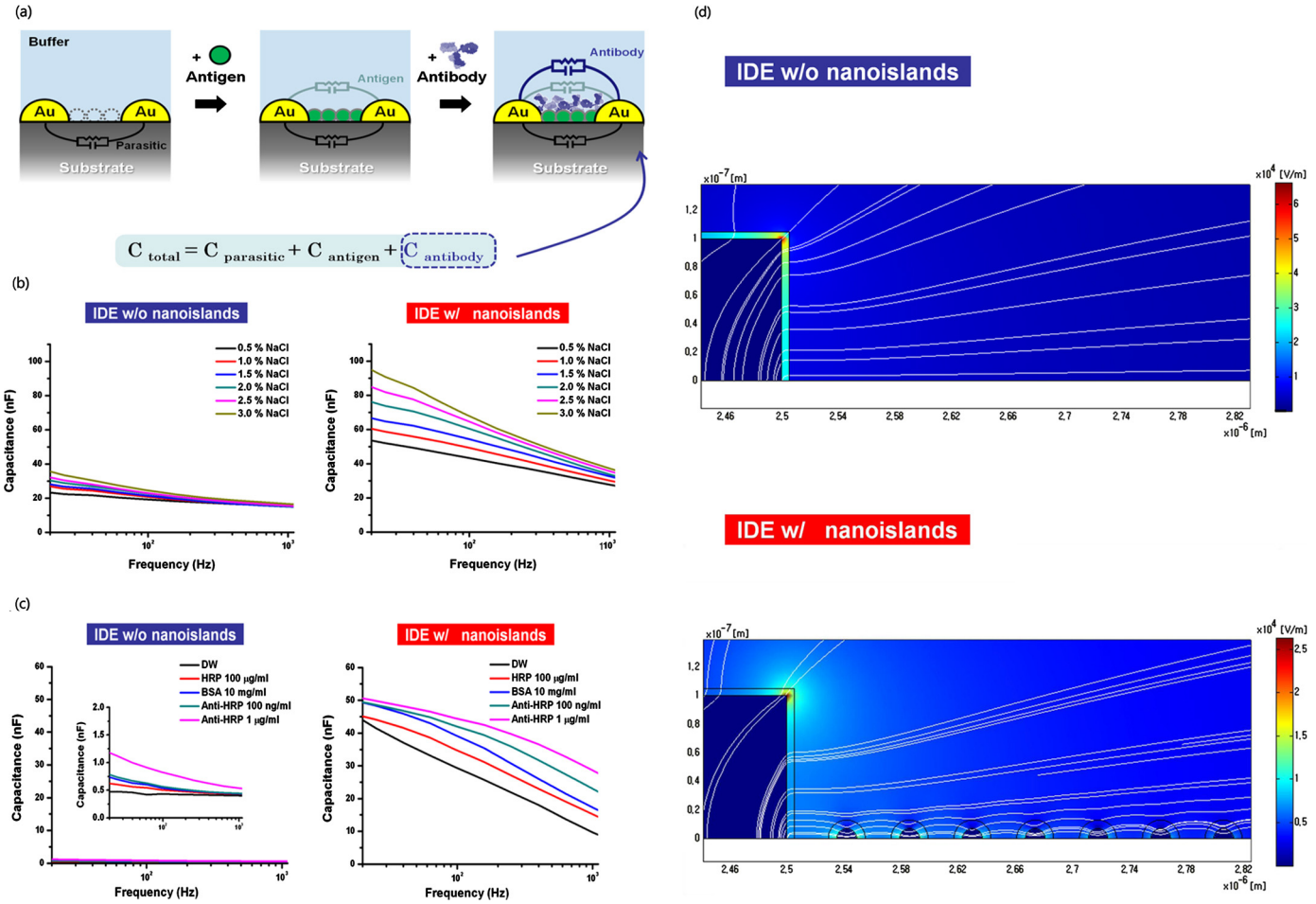

Fig. 2. Immunoassay using the IDE with nanoislands. (a) The principle of the immunoassay based on the IDE with nanoislands. (b) Capacitance change with treatment of standard salt solutions on the IDE without nanoislands (left) and the IDE with nanoislands (right). (c) Capacitive change during the anti-HRP antibody immunoassay using the IDE without nanoislands (left) and the IDE with nanoislands (center). The capacitance change at 100 Hz was of both electrodes was compared (right). (d) Simulated distribution of the electrical fields (color-scaled) and current density (white lines) around a finger of an IDE with a thickness of 100 nm ($\sigma = 10^6$ S m^{-1}, $\varepsilon_r = 1$) covered by a protein layer with a thickness of 5 nm ($\sigma = 10^{-5}$ S m^{-1}, $\varepsilon_r = 20$) immersed in DI water ($\sigma = 10^{-5}$ S m^{-1}, $\varepsilon_r = 80$) (upper) and a finger of the IDE with the protein coated nanoisland array (radius: 7 nm, center to center distance: 44 nm) (lower). The input potential was 10 mV with a frequency of 1 kHz (used Software: COMSOL Multiphysics).

and the relative permittivity (ε_r) of the electrode ($\sigma = 10^6$ S m^{-1}, $\varepsilon_r = 1$), protein ($\sigma = 10^{-5}$ S m^{-1}, $\varepsilon_r = 20$) [33], and medium ($\sigma = 10^{-5}$ S m, $\varepsilon_r = 80$) were isotropic. Furthermore, the whole domain for the electrical fields and the current density was governed by the Laplace equation when neglecting the magnetic field [34]. The simulation results showed the electrical fields distributed on the protein coated nanoislands and the hopping current. Thus, the current response to the input potential reflects the electrical properties of the protein coated on the nanoislands. More research on the hopping current with respect to the distribution and configuration of the nanoislands should be investigated to understand how the nanoislands determine the impedance measurement with the IDE and to improve the label-free IDE sensors.

The electrical characteristic of the typical IDE electrode in the electrolyte can be regarded as interfacial electrode impedance and a serial medium resistance. When the nanoislands were between the IDE fingers, the short-circuiting effect occurred because the flow of current from the adjacent nanoislands with high conductivity was affected. This short-circuiting effect caused not only the change in the impedance but also the sensitivity field of the electrode sensor. It is not yet clear how the equivalent circuit model can be derived considering the short-circuiting effect, which is dependent on the volume and distribution of conductive materials under the electric fields. However, the impedance measured at frequencies below 1 kHz was mostly governed by the interfacial electrode impedance rather than the medium resistance, and therefore could be characterized using a constant phase element or a capacitance model calculated from the imaginary part of the impedance. According to the results illustrated in Fig. 3, an increase in the concentration of electrolyte ions caused an increase in capacitance, which was dependent on the charge density. In the case of the IDE with nanoislands, the capacitance value and also the dependency of the value on the ion concentration was higher than in the normal IDE. This might be caused by an accumulation of the charged ions or an increase in the electrical fields over the nanoislands. The protein was an amphoteric polyelectrolyte which was eager to adsorb onto the surface. The adsorption of the protein caused an increase in the charge density and in the capacitance (see Fig. 2(a)). Although the electrical characteristics of the proteins on the nanoislands can be explained by a complex network of RCs or a transmission line model [35], a simple capacitance model was employed in this study because of the above observation with a limited frequency range.

3.3. Immunoassays with a parylene-A coated electrode

For sensitive immunoassays, receptor molecules (antibodies or antigens) should be immobilized on the sensor surface with a high surface density [26]. For the immobilization of receptor molecules,

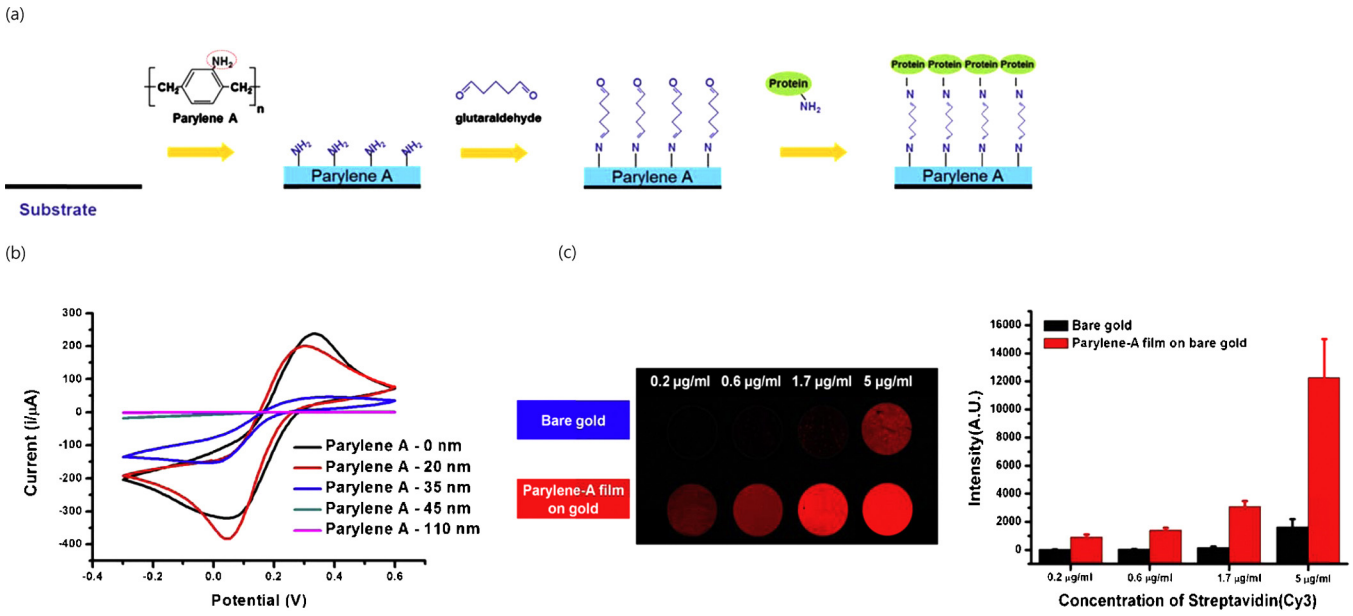

Fig. 3. Characterization of the parylene-A film for protein immobilization. (a) Method of protein immobilization to the parylene-A film. (b) Cyclic voltammetry of a gold electrode coated with a parylene-A film using a redox couple of ferricyanide ($Fe(CN)_6^{3-/4-}$). (c) Comparison of protein immobilization efficiencies to a bare gold surface and a parylene-A film using fluorescence (Cy3)-labeled streptavidin as a model protein. The error bars represent the standard deviation from the mean value ($n = 3$).

SAMs have been used for the functionalization of gold surfaces [1,2,6] and organic silanes have been used for functionalizing oxide surfaces [36]. Such films must be as thin as possible for the highly sensitive capacitive measurement [29]. In this study, a parylene-A film with amine groups was used to immobilize the receptor on the IDE. As previously published [25–27], a parylene-A film can be coated with a thickness less than 100 nm, and it can be used to enhance the sensitivity of immunoassays with a high immobilization efficiency of receptor molecules. As shown in Fig. 3(a), a parylene-A film with amine groups was coated on IDE, and proteins were covalently immobilized to the parylene-A film using glutaraldehyde as a linker molecule.

First, the electrical properties of the parylene-A film were measured using cyclic voltammetry (CV) with ferricyanide as a redox molecule. As shown in Fig. 3(b), the redox peaks of ferricyanide were observed to disappear when the film thickness was more than 45 nm. From the integration of the area of the cyclic voltammogram, the amount of charge transfer was estimated to be 550, 538, 244, 25, and 1.7 mC for a parylene-A film with a thickness of 0, 20, 35, 45, and 110 nm, respectively. These results also showed that the electric isolation steeply increased when the parylene-A film thickness was more than 30 nm. Thus, a parylene-A film less than 30 nm thick was used for the IDE with nanoislands for immunoassay analysis. The immobilization efficiency of the parylene-A film was estimated using fluorescence (Cy3)-labeled streptavidin as a test protein. A fluorescence image was taken after the immobilization of the Cy3-labeled streptavidin to the gold surface and the parylene-A film. As shown in Fig. 3(c), the fluorescence signal of the gold surface was detected at a concentration of more than 5 $\mu g\,mL^{-1}$. However, in the case of the parylene-A film, the fluorescence signal was detected at a concentration of less than 0.2 $\mu g\,mL^{-1}$. These results show that the parylene-A film could improve the limit of detection up to 30-fold by enhancing the efficiency of immobilization.

The parylene-A coated IDE with nanoislands was analyzed with the immunoassay using HRP as a model analyte. First, the capacitive change was measured during the immunoassay using (1) the IDE without nanoislands, (2) the IDE with nanoislands, and (3) the parylene-A coated IDE with nanoislands. In the case of the IDE without nanoislands, the relative capacitive change was estimated at 0.4–0.8 nF (increase ratio = 100%, Δcapacitance = 0.4 nF). Then, the capacitive change was measured to determine the effect of the parylene-A coating. As shown in Fig. 4(a), the relative capacitive change was estimated at 5.6–25.3 nF (increase ratio = 351%, Δcapacitance = 19.7 nF) for the parylene-A coated IDE with nanoislands and at 29.7–44.6 nF (increase ratio = 50%, Δcapacitance = 14.9 nF) for the IDE without a parylene-A coating. These results show (1) that the nanoislands enhanced the sensitivity of the immunoassay more than 30-fold, as evidenced from the comparison of the delta-capacitance values and (2) that a larger capacitance change was observed with the parylene-A film coated on the IDE with nanoislands. The parylene-A coated IDE with nanoislands was analyzed with the capacitive detection of the human hepatitis B virus surface antigen (HBsAg). As with the previous immunoassay with HRP, the capacitance change was measured using the parylene-A coated IDE with nanoislands ($n = 3$). As shown in Fig. 4(b), the limit of detection for the HBsAg was estimated to be 100 $pg\,mL^{-1}$ using the parylene-A coated IDE with nanoislands, and the signal reached a saturation plateau when the sample was treated at a concentration of 1 $\mu g\,mL^{-1}$. When the capacitive change was compared at a frequency of 100 Hz, the relative capacitive change was estimated to be 7.1–19.0 nF (increase ratio = 168%, Δcapacitance = 11.9 nF). At the same time, the impedance change was observed to decrease 66% in the parylene-A coated IDE with nanoislands. As shown in Fig. 4(c), the selectivity of the capacitive biosensor for HBsAg detection was estimated using the antibodies against CRP and hIgG as sample analytes. The sensor responses for these sample analytes (antibodies against CRP and hIgG) were estimated to be insignificant compared with the sensor responses from the samples of anti-HBsAg antibodies. For the applicability test of the capacitive biosensor to real samples, spiked samples of anti-HBsAg antibodies were prepared in human serum ($n = 3$). As shown in Fig. 4(d), the limit of detection for HBsAg was estimated to be 100 $pg\,mL^{-1}$ using the parylene-A coated IDE with nanoislands, and the signal reached a saturation plateau when the samples were treated at a

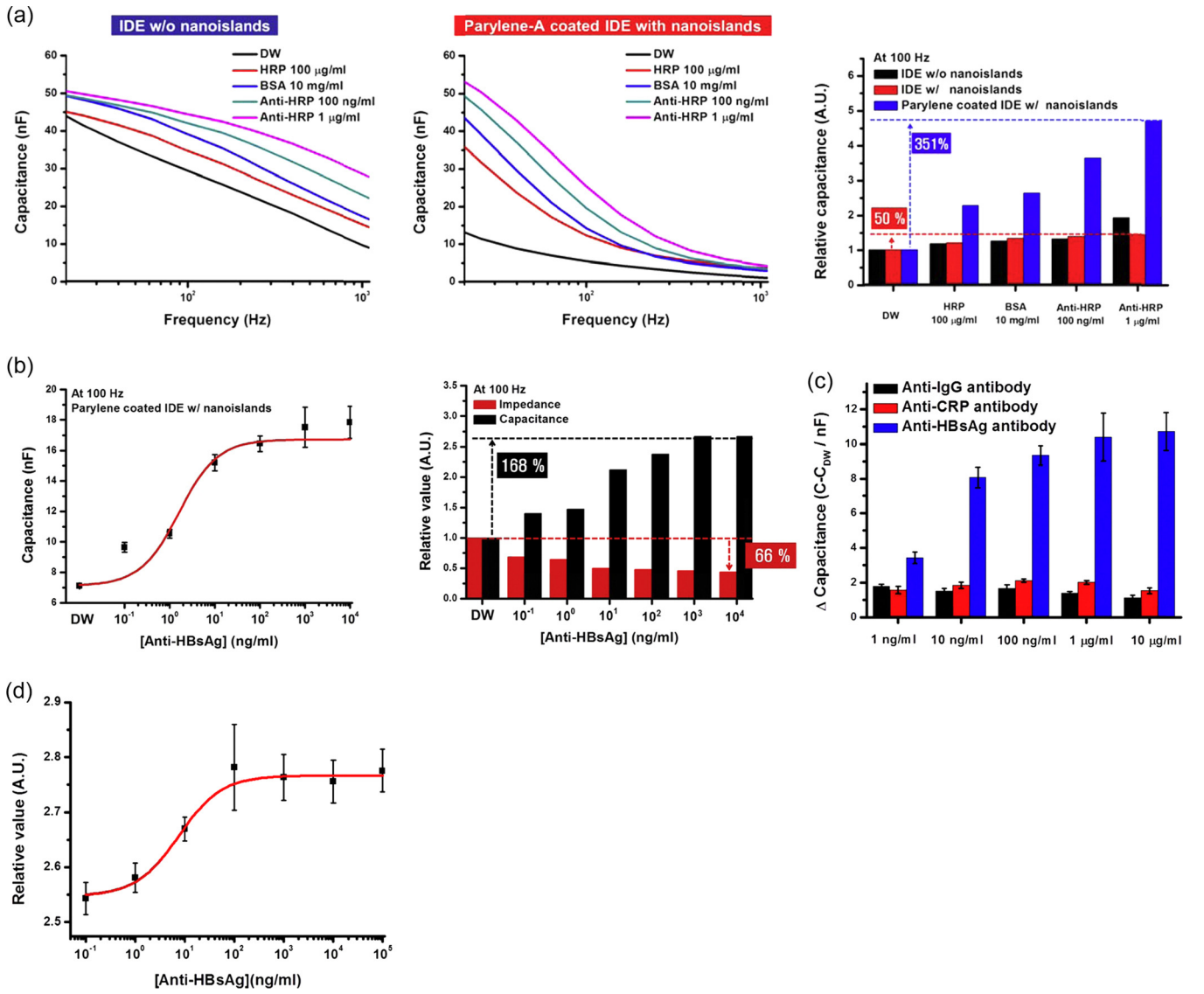

Fig. 4. Immunoassay with the parylene-A coated IDE with nanoislands. (a) Immunoassay with HRP as a model analyte. The capacitive measurement was carried out using the IDE with nanoislands before (left) and after (center) parylene-A coating. The capacitive measurements with different electrodes were compared using relative capacitance (right). (b) Capacitive measurement during the HBsAg immunoassay using the parylene-A coated IDE with nanoislands (left). The capacitive and impedance measurements were compared (right). (c) Selectivity test of the capacitive biosensor for HBsAg detection using antibodies against CRP and hIgG as sample analytes. (d) Applicability test of the capacitive biosensor to real samples with spiked samples of anti-HBsAg antibodies in human serum. The error bars represent the standard deviation from the mean value ($n = 3$).

concentration of 100 ng mL^{-1}. Compared with the samples in PBS (LOD: 100 pg mL^{-1}, saturation concentration: 1 μg mL^{-1}), the LOD was estimated to be at a similar level and the saturation was observed at a 10-fold lower concentration. These results also show that the capacitive biosensor based on the parylene-A coated IDE with nanoislands can be analyzed with the HBsAg immunoassay.

4. Conclusions

A capacitive biosensor based on an interdigitated electrode (IDE) with nanoislands was developed for label-free detection of antigen-antibody interactions. The nanoislands were produced on the IDE to enhance the sensitivity of capacitive detection of protein adsorption. The nanoislands were fabricated on the IDE electrode by (1) deposition of a gold layer with a thickness of 1 nm and (2) thermal treatment. The distribution of nanoislands was estimated to be homogeneous on the electrode surface, with a surface density of 6×10^{11} and 2×10^{11} nanoislands cm^{-2} from AFM and SEM images, respectively. The effect of the nanoislands on the sensitive capacitive measurement was characterized by immunoassay with horseradish peroxidase (HRP) as a model protein. With treatment of standard anti-HRP antibodies, the capacitive change was determined to be from 0.4 to 0.8 nF (Δcapacitance = 0.4 nF) with the IDE without nanoislands and from 29.7 to 44.6 nF (Δcapacitance = 14.9 nF) with the IDE with nanoislands. These results show that the immunoassay using the IDE with nanoislands had a far greater sensitivity than with the IDE without nanoislands. Additionally, a parylene-A film was coated on the IDE with nanoislands to improve the efficiency of protein immobilization. Using fluorescence image analysis, the parylene-A film was determined to improve the limit of detection up to 30-fold by enhancing the efficiency of immobilization. The parylene-A coated IDE with nanoislands was analyzed with immunoassay using HRP as a model analyte. These results showed that (1) the nanoislands enhanced the sensitivity of the immunoassay more than 30-fold, as evidenced by the comparison of the delta-capacitance values and (2) that a larger capacitance change, determined by comparison of the increase ratios, was observed with the parylene-A-coated IDE with nanoislands. Using hepatitis B

virus surface antigen (HBsAg) as a model analyte, the feasibility of use of the parylene-A-coated IDE with nanoislands for medical diagnosis of HBsAg was confirmed.

Acknowledgement

This research was supported by the National Research Foundation of Korea (2013-056267, 2013-056331, 2013-054339 and 2013R1A1A2065723).

Appendix A. Supplementary data

Supplementary data associated with this article can be found, in the online version, at http://dx.doi.org/10.1016/j.aca.2014.07.006.

References

[1] C. Berggren, B. Bjarnason, G. Johansson, An immunological Interleukin-6 capacitive biosensor using perturbation with a potentiostatic step, Biosens. Bioelectron. 13 (1998) 1061–1068.
[2] C. Berggren, P. Stalhandske, J. Brundell, G. Johansson, A feasibility study of a capacitive biosensor for direct detection of DNA hybridization, Electroanalysis 11 (1999) 156–160.
[3] S. Carrara, L. Benini, V. Bhalla, C. Stagni, A. Ferretti, A. Cavallini, B.B. Ricco Samori, New insights for using self-assembly materials to improve the detection stability in label-free DNA-chip and immuno-sensors, Biosens. Bioelectron. 24 (2009) 3425–3429.
[4] M. Bart, E.C.A. Stigter, H.R. Stapert, G.J. de Jong, W.P. van Bennekom, On the response of a label-free interferon-γ immunosensor utilizing electrochemical impedance spectroscopy, Biosens. Bioelectron. 21 (2005) 49–59.
[5] Y.S. Kim, J.H. Niazi, M.B. Gu, Specific detection of oxytetracycline using DNA aptamer-immobilized interdigitated array electrode chip, Anal. Chim. Acta 634 (2009) 250–254.
[6] V.M. Mirsky, M. Riepl, O.S. Wolfbeis, Capacitive monitoring of protein immobilization and antigen–antibody reactions on monomolecular alkylthiol films on gold electrodes, Biosens. Bioelectron. 12 (1997) 977–989.
[7] L. Moreno-Hagelsieb, B. Foultier, G. Laurent, R. Pampin, J. Remacle, J.-P. Raskin, D. Flandre, Electrical detection of DNA hybridization: three extraction techniques based on interdigitated Al/Al_2O_3 capacitors, Biosens. Bioelectron. 22 (2007) 2199–2207.
[8] M. Yi, K.H. Jeong, L.P. Lee, Theoretical and experimental study towards a nanogap dielectric biosensor, Biosens. Bioelectron. 20 (2005) 1320–1326.
[9] S.S. Kallempudi, Y. Gurbuz, A nanostructured-nickel based interdigitated capacitive transducer for biosensor applications, Sensor Actuat. B-Chem. 160 (2011) 891–898.
[10] A. Qureshi, J.H. Niazi, S. Kallempudi, Y. Gurbuz, Label-free capacitive biosensor for sensitive detection of multiple biomarkers using gold interdigitated capacitor arrays, Biosens. Bioelectron. 25 (2010) 2318–2323.
[11] Z. Altintas, S.S. Kallempudi, Y. Gurbuz, Gold nanoparticle modified capacitive sensor platform for multiple marker detection, Talanta 118 (2014) 270–276.
[12] S. Li, H. Cui, Q. Yuan, J. Wu, A. Wadhwa, S. Eda, H. Jiang, AC electrokinetics-enhanced capacitive immunosensor for point-of-care serodiagnosis of infectious diseases, Biosens. Bioelectron. 51 (2014) 437–443.
[13] C. Sontimuang, R. Suedee, F. Dickert, Interdigitated capacitive biosensor based on molecularly imprinted polymer for rapid detection of Hev b1 latex allergen, Anal. Biochem. 410 (2011) 224–233.
[14] J.W. Park, S.S. Kallempudi, J.H. Niazi, Y. Gurbuz, B.S. Youn, M.B. Gu, Rapid and sensitive detection of Nampt (PBEF/visfatin) in human serum using an ssDNA aptamer-based capacitive biosensor, Biosens. Bioelectron. 38 (2012) 233–238.
[15] J.K. Lee, G. Yoo, M. Park, J. Jose, M.J. Kang, J.C. Pyun, Electrochemical ELISA based on *Escherichia coli* with autodisplayed Z-domains, Sensor Actuat. B-Chem. 175 (2012) 46–52.
[16] Z. Zou, J. Kai, M.J. Rust, J. Han, C.H. Ahn, Functionalized nano interdigitated electrodes arrays on polymer with integrated microfluidics for direct bio-affinity sensing using impedimetric measurement, Sensor Actuat. A-Phys. 136 (2007) 518–526.
[17] C. Santschi, M. Jenke, P. Hoffmann, J. Brugger, Interdigitated 50 nm Ti electrode arrays fabricated using XeF_2 enhanced focused ion beam etching, Nanotechnology 17 (2006) 2722–2729.
[18] J. Ahn, T.H. Lee, T. Li, K. Heo, S. Hong, J. Ko, Y. Kim, Y.B. Shin, M.G. Kim, Electrical immunosensor based on a submicron-gap interdigitated electrode and gold enhancement, Biosens. Bioelectron. 26 (2011) 4690–4696.
[19] M.S. Desilva, Y. Zhang, P.J. Hesketh, G.J. Maclay, S.M. Gendel, J.R. Stetter, Impedance based sensing of the specific binding reaction between Staphylococcus enterotoxin B and its antibody on an ultra-thin platinum film, Biosens. Bioelectron. 10 (1995) 675–682.
[20] M. Jung, W.A.E. I-Said, J.W. Choi, Fabrication of gold nanodot arrays on a transparent substrate as a nanobioplatform for label-free visualization of living cells, Nanotechnology 22 (2011) 235–304.
[21] J. Ryu, H.S. Kim, H.T. Hahn, D. Lashmore, Intense pulsed light induced platinum–gold alloy formation on carbon nanotubes for non-enzymatic glucose detection, Biosens. Bioelectron. 25 (2010) 1603–1608.
[22] J.G. Guan, Y.Q. Miao, Q.J. Zhang, Impedimetric biosensors, J. Biosci. Bioeng. 97 (2004) 219–226.
[23] H. Yu, K. Kim, K. Ma, W. Lee, J.W. Choi, C.O. Yun, D. Kim, Enhanced detection of virus particles by nanoisland-based localized surface plasmon resonance, Biosens. Bioelectron. 41 (2013) 249–255.
[24] A.K. Mallia, P.K. Smith, G.T. Hermanson, Immobilized Affinity Ligand Techniques, Academic Press, San Diego, 1992.
[25] B.J. Jeon, M.H. Kim, J.C. Pyun, Parylene-A coated microplate for covalent immobilization of proteins and peptides, J. Immunol. Methods 353 (2010) 44–48.
[26] G. Yoo, M. Park, E.H. Lee, J. Jose, J.C. Pyun, Immobilization of *E. coli* with autodisplayed Z-domains to a surface-modified microplate for immunoassay, Anal. Chim. Acta 707 (2011) 142–147.
[27] H. Ko, G.Y. Lee, B.J. Jeon, J.C. Pyun, Fluorescence immunoassay of anti-cyclic citrulinated peptide (CCP) autoantibodies by using parylene-H film, Biochip J. 5 (2011) 242–245.
[28] E.H. Lee, G. Yoo, M. Park, J. Jose, J.C. Pyun, Optimization of a FACS based-immunoassay using *E. coli* autodisplaying Z-domains, Biochip J. 6 (2012) 231–238.
[29] G.Y. Lee, Y.H. Choi, H.W. Chung, H. Ko, S. Cho, J.C. Pyun, Capacitive immunoaffinity biosensor based on vertically paired ring-electrodes, Biosens. Bioelectron. 40 (2013) 227–232.
[30] B.J. Jeon, M.H. Kim, J.C. Pyun, Application of a functionalized parylene film as a linker layer of SPR biosensor, Sensor Actuat. B-Chem. 154 (2011) 89–95.
[31] P.V. Gerwen, W. Laureyn, W. Laureys, G. Huyberechts, M.O.D. Beeck, K. Baert, J. Suls, W. Sansen, P. Jacobs, L. Hermans, R. Mertens, Dielectrophoretic separation and manipulation of live and heat-treated cells of *Listeria* on microfabricated devices with interdigitated electrodes, Sensor Actuat. B-Chem. 49 (1998) 73–80.
[32] W. Laureyn, D. Nelis, P.V. Gerwen, K. Baert, L. Hermans, R. Magnée, J.-J. Pireaux, G. Maes, DNA hybridization detection on electrical microarrays using coulostatic pulse technique, Sensor Actuat. B-Chem. 68 (2000) 360–370.
[33] S. Grimnes, Ø.G. Martinsen, Bioimpedance and Bioelectricity Basics, second ed., Academic Press, San Diego, 2000.
[34] S. Cho, Electrical impedance simulation and characterization of cell growth using the fricke model, J. Nanosci. Nanotechnol. 12 (2012) 5228–5232.
[35] R. Levie, On porous electrodes in electrolyte solutions: I. Capacitance effects, Electrochim. Acta 8 (1963) 751–780.
[36] Y. Li, L. Syed, J. Liu, D.H. Hua, J. Li, Label-free electrochemical impedance detection of kinase and phosphatase activities using carbon nanofiber nanoelectrode arrays, Anal. Chim. Acta 744 (2012) 45–53.